Journal of Natural Disaster Science, Volume 37, Number 2, 2016, pp67-78

Phreatomagmatic eruptions of 2014 and 2015 in Kuchinoerabujima Volcano triggered by a shallow intrusion of magma

Nobuo Geshi[1], Masato Iguchi[2], and Hiroshi Shinohara[1]

[1] Geological Survey of Japan, AIST
[2] Disaster Prevention Research Institute, Kyoto University,

（Received:Sep 2, 2016 Accepted:Oct.28, 2016）

Abstract

The 2014 and 2015 eruptions of Kuchinoerabujima Volcano followed a ~15-year precursory activation of the hydrothermal system induced by a magma intrusion event. Continuous heat transfer from the degassing magma body heated the hydrothermal system and the increase of the fluid pressure in the hydrothermal system caused fracturing of the unstable edifice, inducing a phreatic explosion. The 2014 eruption occurred from two fissures that traced the eruption fissures formed in the 1931 eruption. The explosive eruption detonated the hydrothermally-altered materials and part of the intruding magma. The rise of fumarolic activities before the past two activities in 1931-35 and 1966-1980 also suggest activation of the hydrothermal system by magmatic intrusions prior to the eruption. The long-lasting precursory activities in Kuchinoerabujima suggest complex processes of the heat transfer from the magma to the hydrothermal system.

Keywords: Kuchinoerabujima Volcano, phreatomagmatic eruption, hydrothermal system, magma intrusion

1. Introduction

Phreatic eruptions are generally caused by the rapid extrusion of geothermal fluid from a hydrothermal system within a volcanic edifice (Barberi et al., 1992). Hydrothermal activities and phreatic eruptions are related to magmatic activities directly or indirectly, as the hydrothermal activities of a volcano are basically driven by heat from magma (Grapes et al., 1974). Many factors such as heat flux from magma and the size of the hydrothermal system affect the activation processes of a hydrothermal system to phreatic eruption (Barberi et al., 1992). Therefore, precise evaluation of activities of the hydrothermal system beneath a volcano is crucial for assessing the risk of phreatic eruption. Risk assessment of phreatic eruption is important particularly for volcanoes situated near areas of human activity, although the scale of phreatic eruptions is relatively small compared to typical magmatic eruptions. A sudden, strong explosion may cause a serious volcanic disaster near the vent area, such as the 2014 Mt. Ontake eruption in Japan (e.g., Kato et al., 2015). Kuchinoerabujima Volcano has experienced repeated phreatic and phreatomagmatic eruptions within the last 100 years (Geshi and Kobayashi, 2007). As the active craters of Kuchinoerabujima Volcano are only 2-3 km from an inhabited area (Fig. 1), such explosive eruptions can cause serious disasters.

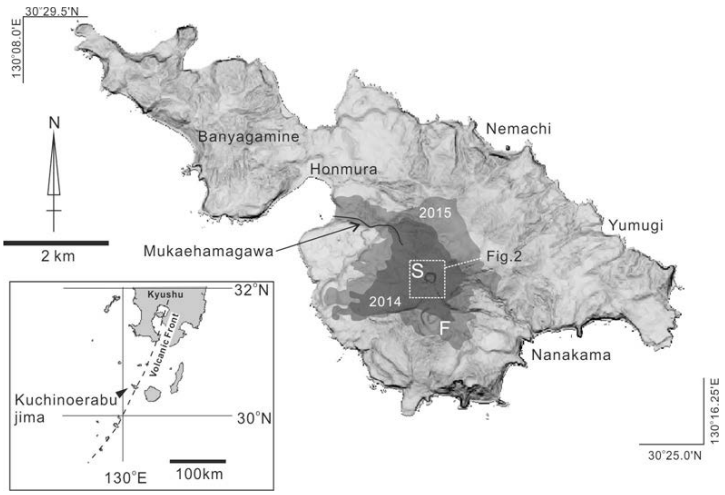

Fig.1 Relief map of Kuchinoerabujima.S: Shindake, F: Furudake. Shadowed areas show the approximate areas of the pyroclastic density current of the August 3, 2014 eruption (2014) and the May 29, 2015 eruption (2015).

The 2014 eruption followed more than 15 years of precursory activities such as the inflation of the edifice, rise of seismicity, and activation of fumarolic activities or hydrothermal systems. This long precursory activity reflects the slow processes of the interactions between the magma and groundwater within the volcano. In this paper, we discuss the process of the activation of the geothermal system by intrusion of the magma body more than 15 years before the eruption.

2. Background of the Kuchinoerabujima Volcano

Kuchinoerabujma Volcano is an active andesitic volcano that sits on the volcanic front of the Ryukyu island arc (Fig. 1). Forming a volcanic island 12 km in length and 38km^2 in area, Kuchinoerabujima Volcano is a cluster of several stratovolcanic edifices that vary in age (Geshi and Kobayashi, 2007). Shindake and Furudake sitting in the central portion of the volcano are the active volcanic centers. The main volcanic edifice of Furudake was formed within the last 15,000 years. Shindake is the youngest volcanic edifice on the island. The main part of Shindake is comprised of andesitic lava flows that erupted ~1000 years ago (Miki et al., 2002; Geshi and Kobayashi, 2007). The Shindake edifice sits on the northwestern slope of Furudake. The development of these explosive breccia and block-and-ash flow deposits indicates the repetition of Vulcanian and phreatomagmatic explosions from the summit craters of Shindake and Furudake. The existence of jointed lava blocks and bread-crust bombs in the explosive breccia indicates the eruption of magmatic materials during the past explosive eruptions.

Records show that the summit crater of Shindake has experienced repeated phreatic and phreatomagmatic eruptions at least since the 19th century. The historical eruptions can be grouped into three active periods: mid-19th century, 1930s, and 1966-1980 (Geshi and Kobayashi, 2007). The last eruption before 2014 occurred on September 28, 1980 from an eruptive fissure ~800 m in the eastern part of the summit of Shindake (Geshi and Kobayashi, 2007). Some major explosions caused serious disasters in the inhabited areas. The strong explosion in 1934 destroyed Nanakama village at the eastern foot of Furudake and killed 8 people.

The presence of a well-developed hydrothermal system within the volcanic edifice is indicated by the geothermal areas and fumaroles in the summit area of Shindake, and the distribution of weak-acid to neutral hot springs along the western and northern coast of the island (Hirabayashi et al., 2002). The electrical resistivity structure detected by the magnetotelluric survey in November 2004 indicates the existence of an aquifer at around 0 – 100 m above sea level in the Shindake edifice (Kanda et al., 2010)

3. Precursory activities to the 2014-2015 eruptions

The 2014 eruption followed a 34-year pause after the 1980 eruption. An inflation of the volcanic edifice centered on Shindake occurred between 1995-96 and 1999 after a low activity period from 1980 (Iguchi et al., 2007). The deformation pattern suggests the existence of an inflation source 0.6 km below the Shindake crater (0.1 km below sea level) (Iguchi et al., 2007). Seismic activity in the shallow part of the volcanic edifice has been active since 1999, following the inflation event. These observations suggest a magma intrusion event and a seismic swarm in 1999 (Iguchi et al., 2007).

Since 1999, seismic activity has maintained a relatively high level. The volcano-tectonic earthquakes concentrate in the shallow part of the Shindake edifice (Triastuty et al., 2009). Seismic activities showed a temporal rise in April of 2001, February 2003, February-March 2004, January 2005, September – October 2006, and September – November 2008. A GNSS station at the northwestern rim of the Shindake crater showed episodic local inflation of the crater area coinciding with the rise of these seismic activities (Saito and Iguchi, 2006; Iguchi et al., 2007).

Fumarolic activities in the summit area of Shindake also activated with the rise of seismic activities and inflation of the volcanic edifice. Fumarolic activities in the Shindake crater have been recognized since 2003 (Iguchi, 2007), gradually spreading from 2003 to 2006. A new vigorous fumarole opened in October 2008 at the southern wall of the main crater (Shinohara et al., 2011). A temporal change of the volcanic gas composition indicates the increase of magmatic gas flux from the period of 2003-2006 to 2009 (Shinohara et al., 2011). In this period, remarkable demagnetization in the shallow part of the Shindake crater was detected (Kanda, 2007; Kanda et al., 2010). Following this rise in volcanic activities, explosive eruptions occurred from the Shindake summit crater on August 3, 2014 and May-June 2015.

4. The 2014 eruption

4.1 Outline

The 2014 eruption occurred at around 12:24 local time on August 3 (Japan Meteorological Agency, 2014). The eruption occurred at the summit of Shindake. The eruption column reached ~800 m above the crater and drifted in the NNE direction. Ballistic blocks are scattered mainly in the north and south directions and reached an area within ~1 km of the summit crater. At the same time, the pyroclastic density current (PDC) flowed down from the summit area and reached the coastal line, ~2.2 km from the summit crater (Fig. 1).

4.2 Eruptive fissures

The August 3 eruption formed two eruptive fissures at the summit of Shindake (Fig. 2(a) and (b)). A north-south trending fissure (fissure "E") ~500 m in length and a maximum 40 m in width opened along the eastern rim of the main summit crater (Fig. 2(a)). This eruption fissure separated into the northern segment (fissure "En") and southern segment (fissure "Es"). The southern end of Fissure Es curves westward at the foot of Furudake. Fissure E is almost parallel to the eruptive fissure of the 1945 and 1980 eruptions on the upper eastern slope of Shindake. Another eruptive fissure (fissure "W") is a NE – SW trending fissure ~400 m in length. Fissure W developed from the center of the summit crater to the upper part of the western slope of Shindake (Fig. 2(a)). The summit crater of Shindake was half buried by the ejecta from these fissures.

Vigorous fumarolic activity was observed at the center of Fissure W after the 2014 eruption. The location of the fumarole in the fissure corresponds to the western margin of the central crater, where weak fumarolic activity was observed prior to the eruption. The amount of SO_2 gas emission reached 1000 – 4600 ton/day after the 2014 eruption (Japan Meteorological Agency, 2015).

The locations of these eruption fissures of the 2014 eruption trace the fissures of the 1931 eruption (Tanakadate, 1938). The eruption fissures En and Es of the 2014 eruption traced the F1 and F3 of the 1931 eruption (Tanakadate, 1938). The location of the eruption fissure W coincides with that of the G-S-S2 crater chain of the 1931 eruption (Tanakadate, 1938) (Fig. 2(c)).

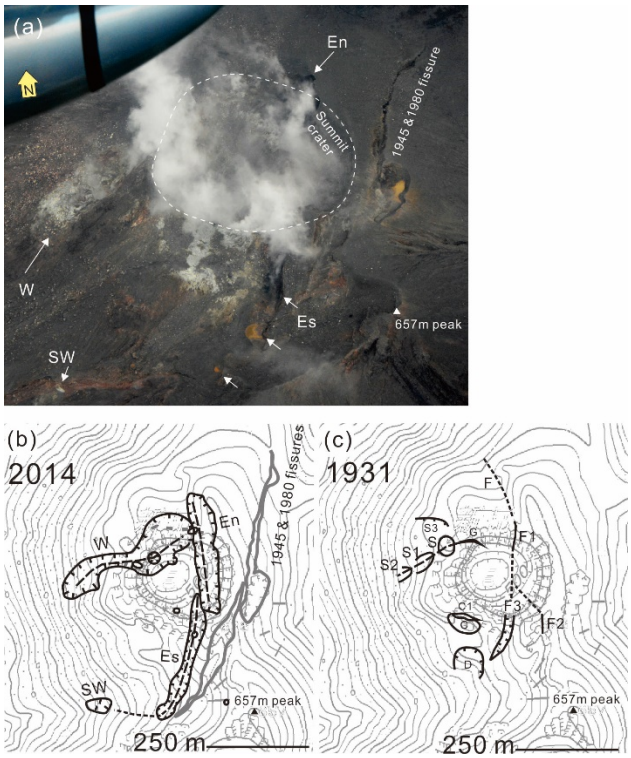

Fig. 2. (a) Sub-vertical aerial photo of the summit of Kuchinoerabujima after the 2014 eruption taken on October 2, 2014. The eruption fissures formed during the 2014 eruption (En, Es, W and SW) are indicated by arrows.
(b) Illustrations of the distribution of the eruption fissure formed by the 2014 eruption.
(c) Distribution of the eruption fissures and craters of the 1931 eruption (Tanakadate, 1938). The structure is named after Tanakadate (1938). F-F1 and G-S-S1-S2 were formed by the explosion on April 2, 1931. The explosion on May 15 formed craters C, D and F3.

4.3 Erupted materials

Method

The ash samples were washed by an ultrasonic cleaner to remove fine grains less than ~0.1 mm. The samples were dried and sieved into groups >1 mm, 1-0.5 mm, 0.5-0.25 mm, 0.25-0.125 mm, and less than 0.125 mm in diameter. The samples between 0.5-1.0 mm and 0.25-0.5 mm were used for the grain component analysis. The sieved grains were divided into several groups based on their external characteristics (shape, color, texture) under an optical microscope.

Ash grains were included in epoxy resin and polished to analyze the interior texture and chemical composition. “Non-altered glassy grains” were picked up manually and included in the resin and polished. The chemical composition of the interstitial glass was determined with an energy dispersive X-ray spectrometer (X-Max 20 with INCA software of Oxford Instruments) on a Scanning Electron Microscope (SEM, JEOL JSM-6610LV) of the Geological Survey of Japan, AIST. The probe conditions were 15 kV and ~1.0 nA. Each chemical analysis was conducted in a rectangle area with the sample having a polished surface of more than 100 μm^2. All elements detected by EDS were quantified. The water contents were estimated from the difference between the total amount of oxygen detected by EDS and the stoichiometric amount of oxygen to form all detected elements as oxide.

Results

The ash samples for component analysis were collected from the air-fall deposit in the northern part of the

island. The 2014 eruption produced pyroclastic materials consisting of a mixture of various types of rock fragments (Fig. 3(a)). The volcanic ash consisted of grayish-colored microcrystalline lava fragments (~50%), yellowish – reddish brown rock fragments (~10-20%), and whitish-colored hydrothermally-altered rock fragments (~10-20 %). Additionally, small amounts of "non-altered glassy grains" were recognized (~10%). These grains exhibited a semi-transparent grayish color with a glossy surface under an optical microscope (Fig. 3(b)). The grains had an angular outline surrounded by a brittle-fractured surface (Fig. 3(c)). A smooth and fluidal surface was also recognized in part of some grains (Fig. 3(d)). Some grains had microcracks on the surface (Fig. 3(e)). The grains also contained vesicles with an irregular shape up to 30 vol.%.

The interior of the glassy fragments consists of interstitial glass, plagioclase, pyroxene, iron-titanium oxide and silica mineral as groundmass crystal (Fig. 3(f)), in addition to the phenocryst-size crystals (crystals larger than the grain size). Groundmass minerals exhibit a euhedral-subhedral shape. Silica minerals exhibit an elongated euhedral shape surrounded by the interstitial glass. Interstitial glass has a rhyolitic composition with 77.3±0.3 wt.% of SiO_2 (water-free value). The crystallinity of groundmass in the grains ranges from 60 -90%. The estimated water concentration in the groundmass glass ranges from 1.2 to 1.6 wt.%.

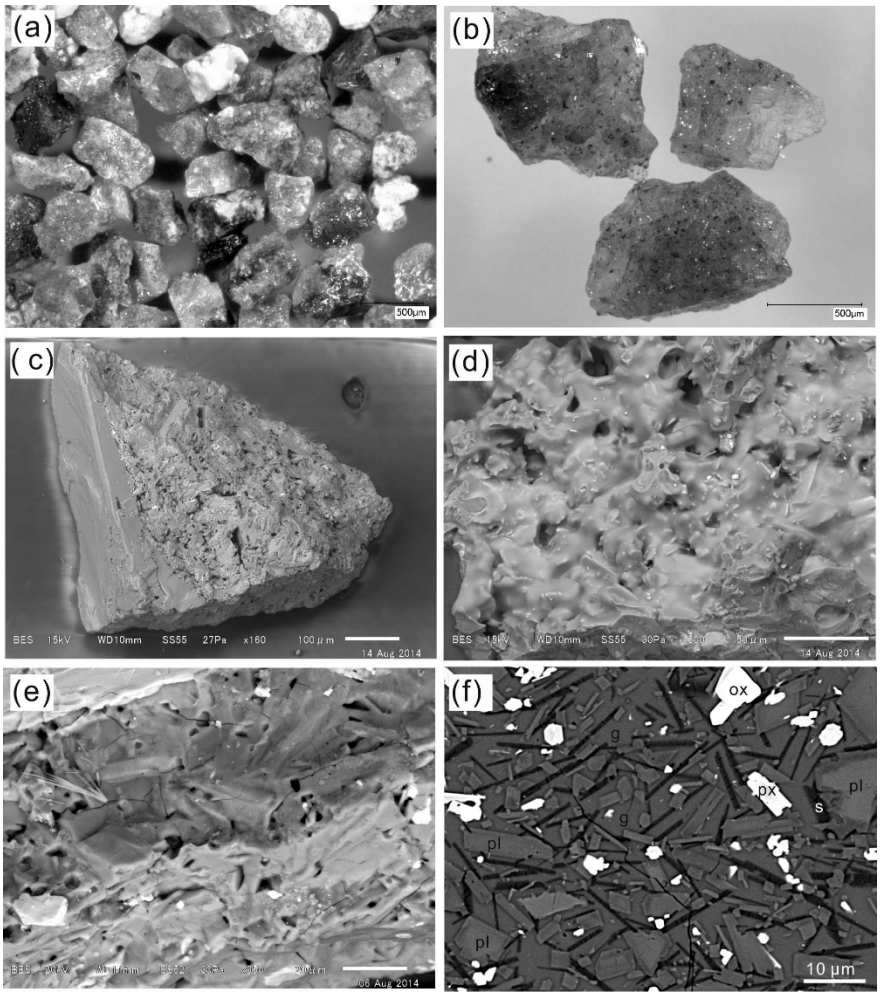

Fig. 3. Ash grains of the 2014 tephra. (a) optical image of the grains, (b) separated juvenile grains, (c) Scanning Electron Microprobe (SEM) image of the juvenile grains, (d) fluidal surface of the juvenile grains, (e) micro-cracks on the juvenile grain, (f) back-scattered electron image of the interior of the juvenile grains. Pl: plagioclase, px: pyroxene, ox: iron-titanium oxide, s: silica minerals, and g: interstitial glass.

5. The 2015 eruption

5.1 Outline

The 2015 eruption consisted of two explosive events that occurred on May 29 and June 18. The May 29 eruption occurred at 9:59 from the central part of the summit crater of Shindake (Japan Meteorological Agency, 2015, Uhira and Toriyama, 2015). The eruption column reached >9 km above the crater and drifted southeastward. Ash fall covered the southern half of Yakushima Island, 20-40 km east of the Shindake crater. Ballistic blocks reached an area within ~2 km of the summit crater, some of which caused minor forest fires. PDC flowed down from the summit area in all directions and covered a larger area compared to the PDC of the 2014 eruption (Fig. 1). The maximum lobe of the PDC flowed northwestward and reached the coastline, ~2.2 km from the summit crater. Strong explosive activity lasted within 10 minutes, followed by low and continuous emission of steam (Uhira and Toriyama, 2015).

The June 18 eruption occurred at 12:17 from the summit crater of Shindake (Japan Meteorological Agency, 2015). Owing to the bad weather conditions, details of the eruption are unknown. The eruption cloud drifted northeastward. Lapilli fall was observed on a ship at ~9 km off Kuchinoerabujima. Ash fall distributed in the northern part of Yakushima and Tanegashima. Minor ash emissions were also observed on June 19.

5.2 Eruption site

The 2015 eruptions occurred from the bottom of the Shindake summit crater (Japan Meteorological Agency, 2015). The depth of the Shindake crater increased after the eruption, although no significant change of the horizontal outline of the crater was observed. The fractures formed in the 2014 eruption remained after the 2015 eruption, although part of the fissures outside of the Shindake summit crater were buried by the debris ejected during the 2015 eruption (Fig. 4).

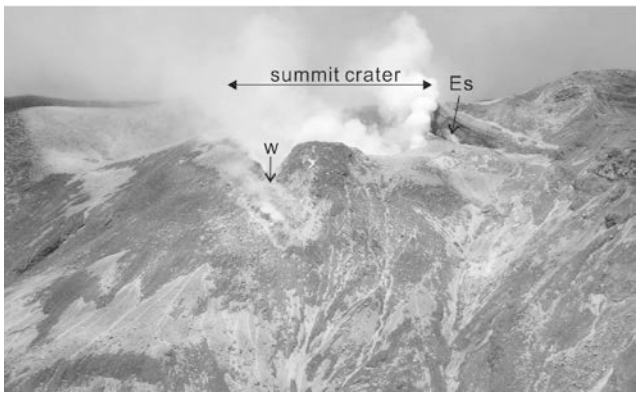

Fig. 4. The summit area after the 2014 eruption taken on 1 June, 2015, by R. Kazahaya.

5.3 Erupted materials

We observed the samples of ash fall deposit collected in the western part of Yakushima Island and the ash samples collected at the marginal part of the PDC. The procedures of the sample preparation and analysis are the same as the samples of the 2014 eruption (described in 4.3).

The components of the erupted materials in 2015 are similar to that of the 2014 eruption. The volcanic ash consists of grayish-colored microcrystalline lava fragments (~40%), yellowish – reddish brown rock fragments (~20-30%), and whitish-colored hydrothermally-altered rock fragments (~10-20%). A small amount of non-altered grains was also recognized in the tephra of the May 29 and June 18 eruptions. These grains exhibited a grayish color and had a semi-transparent and glossy surface under an optical

microscope (Fig. 5a)). The grains had an angular outline surrounded by brittle-fractured surfaces (Fig. 5(b)). Very-few grains with a smooth and fluidal surface were recognized. Some grains also had microcracks on the surface (Fig. 5(c)). The vesicularity of these glassy grains was less than 30%.

The interior of these glassy fragments consists of plagioclase, pyroxene, iron-titanium oxide and silica mineral as groundmass crystal, in addition to phenocryst-size crystals (crystals larger than the grain size). The glassy fragments are almost crystallized and contained a very minor amount of interstitial glass (Fig. 5(d)). Due to the very narrow space of the interstitial glass, we could not analyze the chemical composition of the interstitial glass.

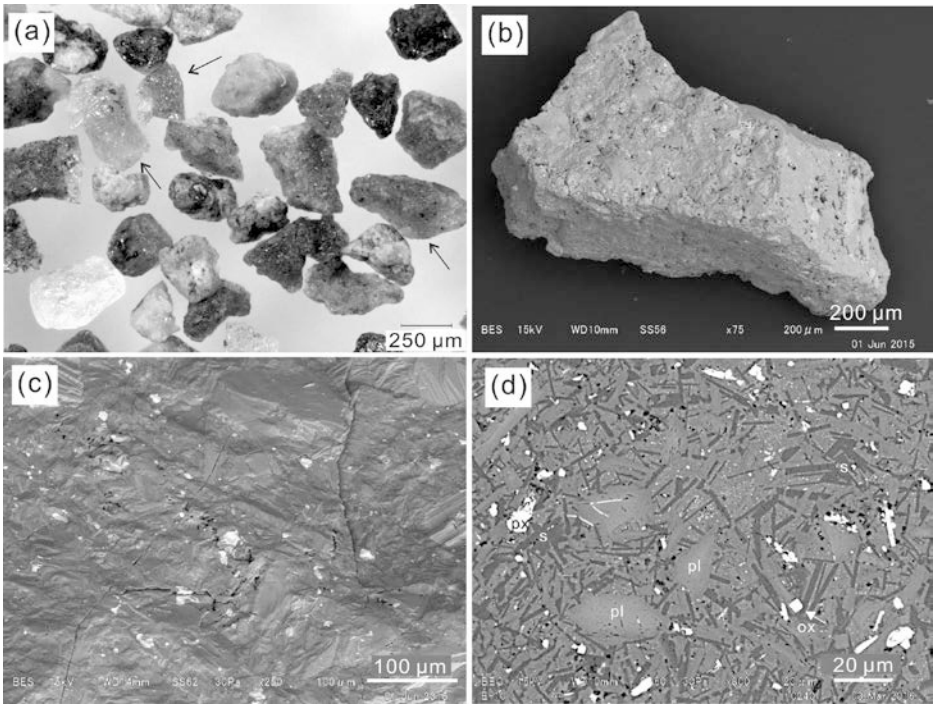

Fig. 5. Ash grains of the 29 May eruption in 2015. (a) optical image of the grains (arrows indicate fresh grains), (b) SEM image of a fresh glassy grain, (c) micro-cracks on the fresh grain, (d) back-scattered electron image of the interior of the fresh glassy grains. Pl: plagioclase, px: pyroxene, ox: iron-titanium oxide and s: silica minerals.

6. Comparison with the past eruptions

Two activated periods in 1931–1945 and 1966-1980 separated by relatively-low activity periods were recognized during the last ~100 years before the activation in 1999. During the activated period, several explosive eruptions occurred. Phreatic eruptions occurred in 1945 and 1980 at the end of the activated period.

The records show the activation of fumarole prior to the major eruptions in 1931 and 1966 (Fig. 6). Prior to the activated period of 1931-1945, a new fumarole appeared in 1914 and sulfur mining was in operation until the 1931-1945 eruptions (Tanakadate, 1938). The activation of fumarolic activities from the Shindake summit crater before the 1966 eruption was also documented (Kagoshima Meteorological Observatory and Fukuoka Meteorological Observatory, 1967).

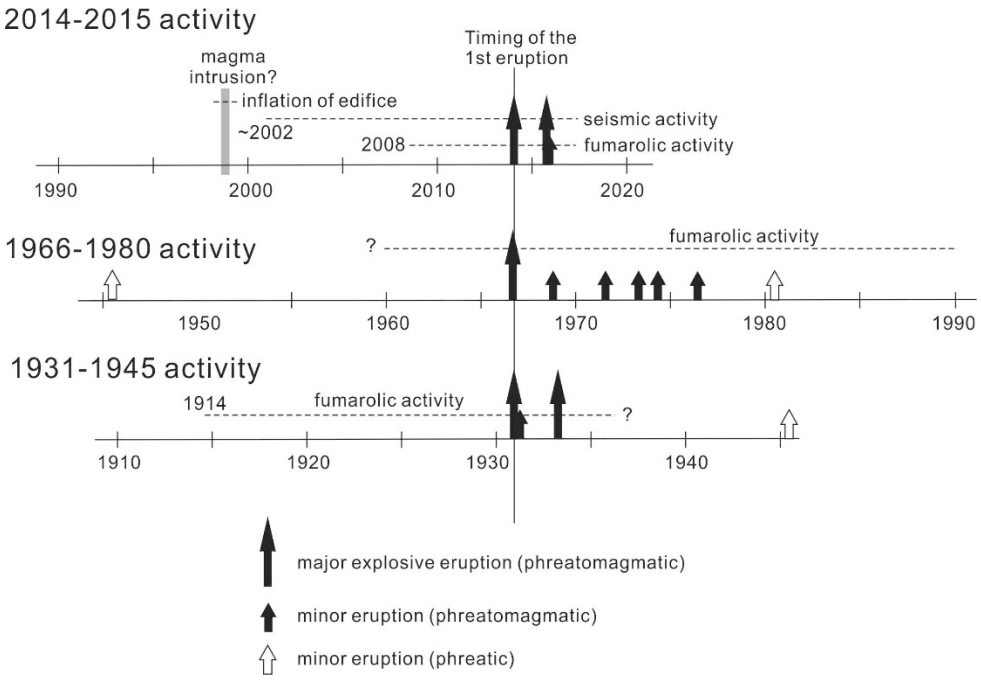

Fig. 6. Time evolution of the 2014-2015 activities in comparison with the 1966-80 and 1931-1945 activities.

The development pattern of eruptive vents in the 1931-1934 eruptions is similar to that in the 2014-2015 eruption (Figs. 2(b) and (c)). The first eruption on April 2, 1931, occurred from two fissures: one is the E-W trending fissure from the center of the summit crater to the western rim, and the other is the N-S trending fissure from the center of the crater to the southern rim (Tanakadate, 1938), as the eruption on August 3, 2014. The position of these eruptions coincides with that of the 2014 eruption. The following eruptions in 1931-1934 occurred from the center of the summit crater (May 29 and June 18 eruptions in 2015, and May 15, June 6 in 1931, and eruptions in 1933-1934).

The ejection of high-temperature blocks was also recognized in the 1931, 1933-34, and 1966 eruptions. These high-temperature blocks caused fires in Nanakama village on the eastern flank of the volcano in the eruption on December 24, 1933 (Tanakadate, 1938). The landing of ballistic blocks during the eruption on November 22, 1966 also caused several forest fires on the northern slope of the volcano (Kagoshima Meteorological Observatory and Fukuoka Meteorological Observatory, 1967). The tephra of the 1966 eruption contains several fresh glassy fragments that are juvenile materials. Several jointed blocks of the 1966 eruption were also found in the summit area of Shindake (Geshi and Kobayashi, 2007). The evidence of the ejection of high-temperature blocks during the past eruptions suggests the existence of shallow intrusions of magma.

7. Discussions

7.1 Heat source of the precursory hydrothermal activation

The identification of magmatic juvenile materials and examination of their petrological characteristics are fundamental to understanding what triggers eruptions. However, such identification is difficult in the case of Kuchinoerabujima, because of the narrow variation in the petrological characteristics of the magma during the last ~10,000 years (Geshi and Kobayashi, 2007). Most of the crater wall consists of thick andesitic lava (Shindake Lava: Geshi and Kobayashi, 2007). The interior of andesitic lava was crystallized

during slow cooling and no interstitial glass remained. The presence of interstitial glass in grains indicates the rapid cooling of magmatic materials during the eruption. The absence of alteration is also an indicator of juvenile magmatic materials. The ejecta of the past eruptions on the summit are suffered from alteration and weathering in various degrees owing to the fumarolic activities in and around the summit area. Volcanic glass is easily affected by the hydrothermal alteration and the surface of the glass loses its freshness. Therefore, the characteristics of the fresh glassy grains in the tephra of the 2014 and 2015 eruptions, such as the absence of the hydrothermal alteration, presence of fresh interstitial glass in the grains and the development of chilled fractures on the surface, indicate that they are magmatic (juvenile) materials quenched at the timing of eruption.

The fluidal-shaped surface and the presence of interstitial glass in the juvenile grains of the 2014 eruption indicate that these grains were still in a partially-molten state at the eruption. In contrast, the very-minor volume of interstitial glass in the grains in the 2015 volcanic ash suggests the progress of crystallization of magma to the 2015 eruption.

The petrological investigations on the juvenile materials reveal the settling condition of magma. The mineral assemblage in their groundmass, particularly the presence of silica minerals, suggests the crystallization in a low-pressure condition less than 10 MPa (I. Miyagi, personal communication). Estimated water contents in the groundmass glass (1.2-1.6 wt.%) also correspond to the water solubility in rhyolitic melt at 10 -20 MPa (Burgisser, et al., 2010). These pressures correspond to the lithostatic pressure at a depth of ~0.5-1 km, assuming that the density of the volcanic edifice is 2000 kgm^{-3}. The chemical composition of fumarolic gas also suggests the degassing under low pressure (Shinohara et al., 2011). The estimated depth coincides with the depth of the inflation source between 1995/96 and 1999 (Iguchi et al., 2007). These observations support the idea that the inflation event between 1995/96 and 1999 was caused by a magmatic intrusion at a shallow depth. The intruding magma body was kept in a molten state during the precursory stage and heated the hydrothermal system by the supply of volcanic gas. The absence of a remarkable inflation event at the depth of ~1-2 km after the inflation event between 1995/96 and 1999 (Saito and Iguchi, 2006) indicates that no major additional intrusion occurred after 1999. The high crystallinity and low vesicularity of the juvenile materials in the 2014 eruption indicate the effective degassing and outgassing of volatile components from the magma prior to the eruption. The increase of crystallinity in the groundmass from the 2014 eruption to the 2015 eruption can reflect the vigorous outgassing from the magma observed between the two eruptions.

The phreatomagmatic explosions triggered by the long-term outgassing from an intrusive body also occurred in the past eruptions (Fig. 6). The records of sulfur mining in Shindake show that the eruptions in 1931-34 were preceded by remarkable fumarolic activity from 1914. The active degassing from Shindake was also recognized prior to the 1966 eruption. The presence of high-temperature blocks during these eruptions indicates the ejection of “magmatic” materials, suggesting the existence of a shallow intrusive body. The fumarolic activities before the eruptions are caused by the outgassing from intrusive bodies. These examples suggest that the activation of the hydrothermal system can take more than 10 years in the case of Kuchinoerabujima.

7.2 Fracturing of the edifice

A direct trigger is required for a sudden explosion during the long-term activation of the hydrothermal system. The fragments of hydrothermally-altered host rock in the 2014 ejecta suggest an explosion from the shallow hydrothermal system, although the ejecta contain a small volume of juvenile grains. The development of the eruption fissures during the 2014 eruption (Fig. 2) indicates a major fracturing of the volcanic edifice. Intermittent inflation of the Shindake edifice prior to the eruption (Saito and Iguchi, 2006; Shinohara et al., 2011) indicates the increase in fluid pressure in the hydrothermal system. The rise of the fluid pressure in the hydrothermal system resulted in the fracturing of the edifice to induce phreatic explosion in the hydrothermal system (Fig. 7). Once a fracture destroys the cap rock and reaches a pressurized hydrothermal system, the fractures may cause rapid decompression of the hydrothermal system in the edifice (Barberi et al., 1992). Decompression of the pressurized hydrothermal fluid triggered the rapid phase change to vapor and consequently induced the steam explosion of “phase-equilibrium type

destruction" (Taniguchi, 1996) through the fractures. The similarity of the development of eruption fissures in the 1931 eruptions to that in the 2014 eruption suggests that the 1931 eruptions were also triggered by the fracturing of the volcanic edifice with an activated hydrothermal system. The explosion involved part of the intruding magma beneath the hydrothermal system and produced the juvenile grains (Fig. 3). The low vesicularity and high crystallinity of the juvenile grains indicate (Fig. 3) that the fragmentation of the juvenile grains was mainly driven by a passive process with rapid decompression of the solidifying magma rather than the expansion of vesicles in magma.

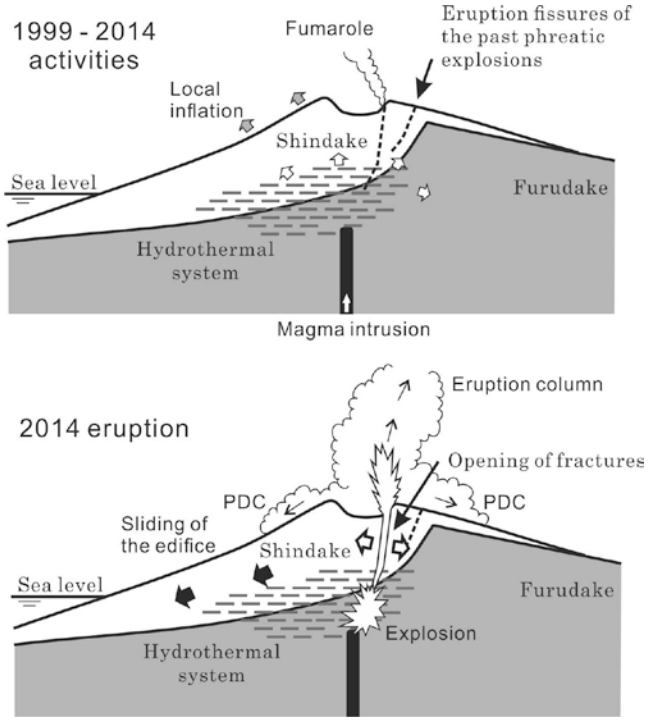

Fig. 7 Schematic illustrations of the precursory stage (1999 – 2014) and the phreatic explosion in the 2014 eruption. During the precursory stage, the hydrothermal system is heated by the intrusion. Expansion of the hydrothermal system caused the local inflation of the summit area. Part of the hydrothermal fluid is released through the fracture and formed fumarole. During the 2014 eruption, a fracture cut the hydrothermal system inducing rapid decompression of the hydrothermal system and the phreatic explosion.

The structural instability of the Shindake edifice may promote the fracturing in the Shindake edifice. As the volcanic edifice of Shindake sits on the western slope of the ridge between Furudake and Noike (Geshi and Kobayashi, 2007), an E-W extended stress acts on the upper portion of the edifice. The parallel development of several eruption fissures in the 1931, 1945, 1980 and 2014 eruptions (Tanakadate, 1938, Geshi and Kobayashi, 2007) indicates the fracturing of the edifice by the westward sliding of the Shindake edifice. The E-W extension of the volcanic edifice is also indicated by the focal mechanisms of the earthquakes in Shindake (Triastuty et al., 2009). The rise of seismic activity prior to the 2015 eruption also suggests fracturing within the edifice. Because the seismic activities before the 2015 eruption distribute mainly below sea level (Japan Meteorological Agency, 2015), the structural instability of the edifice is not the direct trigger for these seismic activities and eruption. As the deformation and fracturing of the Shindake edifice triggers the phreatic explosive activities, the monitoring of the deformation of the edifice is useful for the evaluation of potential phreatic explosion in Kuchinoerabujima Volcano.

8. Conclusions

The important processes of the phreatomagmatic explosive activities in Kuchinoerabujima Volcano are the heating of the hydrothermal system by shallow intrusion as a precursory stage and the formation of open fractures by the instability of the edifice as a direct trigger of explosion. The precursory activities for the 2014 and 2015 eruptions indicate the gradual activation of the hydrothermal system by the intrusion of magma ~15 years prior to the eruption. The intruding magma between 1995 and 1999 was still molten at the 2014 eruption and released volatiles into the hydrothermal system for ~15 years. The hydrothermal system was gradually heated by the input of heat and volatiles from the magma.

Fracturing of the volcanic edifice may trigger the rapid decompression of the hydrothermal fluid, resulting in the phreatic explosion in the 2014 eruption. Part of the intruding magma was also involved in the explosion and ejected as the quenched juvenile grains.

The similarity of the precursory process of the 2014-2015 eruptions to that of the previous eruptions in 1931-45 and 1966-1980 suggests that the previous eruptions were also induced by the magma intrusion and the activation of the hydrothermal system can take more than 10 years to erupt.

Acknowledgements

The ash samples for analysis were collected and provided by Japan Meteorological Agency (2014 and 2015 tephra) and Mr. Shojiro Nakagawa (2015 tephra). Analysis of ash grains was supported by I. Miyagi, A. Tomiya, G. Miwa and M. Nagai. We are grateful to the two anonymous reviewers for their constructive comments and suggestions.

References

Barberi, F., Bertagnini, A., Landi, P. and Principe, C., 1992. A review on phreatic eruptions and their precursors. Jour. Volcanol. Geotherm. Res., 52, 231-246.

Burgisser, A., Poussineau, S., Arbaret, L., Druitt, T.H., Giachetti, T. and Bourdier, J-L., 2010. Pre-explosive conduit conditions of the 1997 Vulcanian explosions at Soufrière Hills Volcano, Montserrat: I. Pressure and vesicularity distributions. Jour. Volcanol. Geotherm. Res. Vol. 194, pp. 27-41. 2010.

Geshi, N. and Kobayashi, T. 2007. Geological Map of Kuchinoerabujima Volcano (1:25,000). Geological Map of Volcanoes 14, Geological Survey of Japan, AIST.

Grapes, R.H., Reid, D.L. and McPherson, J.G., 1974. Shallow dolerite intrusion and phreatic eruption in the Allan Hills region, Antarctica. New Zealand Jour. Geology Geophysi., 17, 563-577.

Hirabayashi, J., Nogami, K., Suzuki, T. and Mizubayashi, M., 2002. Volcanic gas and hot springs of Kuchinoerabu-jima. Report on Joint Observation at Satsuma-Iwojima and Kuchinoerabujima Volcanoes 2000. DPRI, Kyoto University, 143–152.

Iguchi, M., 2007. Detection of change of anomalous geothermal area by aerial infrared thermal measurements at Kuchinoerabujima Volcano. DPRI, Kyoto Univ, 53-58.

Iguchi, M., Saito, E., and Suzuki, A., 2007. Repeated GPS measurements at Kuchinoerabujima Volcano during the period from 1995 to 2006, DPRI. Kyoto Univ. 33-40.

Japan Meteorological Agency, 2014. Major eruptive activities in Japan in 2014, in "Monthly report on earthquakes and volcanoes in Japan, December 2014" 118-128.

Japan Meteorological Agency, 2015. Major eruptive activities in Japan in 2015, in "Monthly report on earthquakes and volcanoes in Japan, December 2015" 98-110.

Kagoshima Meteorological Observatory and Fukuoka Meteorological Observatory, 1967. Report on the explosion of Shindake, Kuchinoerabujima Island on November 22, 1966. Memories of Fukuoka Meteorological Observatory, 22, 79-98.

Kanda, W., 2007. Recent geomagnetic field variations observed at Kuchi-erabu-jima Volcano. DPRI, Kyoto Univ. 17-24.

Kanda, W., Utsugi, M., Tanaka, Y., Hashimoto, T., Fujii, I., Hasenaka, T. and Shigeno, N., 2010. A heating process of Kuchi-erabu-jima Volcano, Japan, as inferred from geomagnetic field variations and electrical structure. Jour. Volcanol. Geotherm. Res. 189, 158-171.

Kato, A., Terakawa, T., Yamanaka, Y., Maeda, Y., Horikawa, S., Matsuhiro, K., and Okuda, T., 2015. Preparatory and precursory processes leading up to the 2014 phreatic eruption of Mount Ontake, Japan. Earth, Planets Space 67, DOI: 10.1186/s40623-015-0288-x.

Miki, D., Iguchi, M., Eto, T., Solihin, A., 2002. Paleomagnetic ages of the lava flows of Shindake, Kuchinoerabujima. DPRI, Kyoto Univ. 159-168.

Saito, E., and Iguchi, M., 2006. Ground deformation detection at Kuchinoerabujima Volcano by continuous GPS with simple atmospheric correction. Bull. Volcanol. Soc. Japan, 51, 21-30.

Shinohara, H., Hirabayashi, J. and Iguchi, M., 2011. Evolution of volcanic gas composition during repeated culmination of volcanic activity at Kuchinoerabujima Volcano. Japan. Jour. Volcanol. Geotherm. Res., 202, 107-116.

Tanakadate, S., 1938. Eruptions of Shindake on Kuchinoerabujima: morphology of the crater and debris avalanches on Mukae-hama. Bull Volcanol Sco Japan, 4, 339-354.

Taniguchi, H., 1996. Mechanism of a phreatomagmatic explosion due to the interaction between hot rhyolitic lava flow and external water. Mem. Geol. Soc. Japan, 46, 149-162.

Triastuty, H., Iguchi, M. and Tameguri, T., 2009. Temporal change of characteristics of shallow volcano-tectonic earthquakes associated with increase in volcanic activity at Kuchinoerabujima Volcano. Japan. Jour. Volcanol. Geotherm. Res. 187, 1–12.

Uhira, K. and Toriyama, N., 2015. Meeting with the May 29, 2015, eruption of Kuchinoerabujima volcano. Bull. Volc. Soc. Japan, 60, 487-490.